RESEARCH ARTICLE

FASEB BioAdvances   WILEY

Transcriptome analysis of the zebrafish *atoh7−/−* Mutant, *lakritz*, highlights Atoh7-dependent genetic networks with potential implications for human eye diseases

Giuseppina Covello[1] | Fernando J. Rossello[2] | Michele Filosi[1] | Felipe Gajardo[3] | Anne-Laure Duchemin[4] | Beatrice F. Tremonti[1] | Michael Eichenlaub[2] | Jose M. Polo[2,6] | David Powell[7] | John Ngai[8] | Miguel L. Allende[3] | Enrico Domenici[1,5] | Mirana Ramialison[2] | Lucia Poggi[1,4,9]

[1]Department of Cellular, Computational and Integrative Biology - CIBIO, University of Trento, Trento, Italy

[2]Australian Regenerative Medicine Institute, Monash University Clayton VIC, Clayton, Australia

[3]Center for Genome Regulation, Facultad de Ciencias, Santiago, Universidad de Chile, Santiago, Chile

[4]Centre for Organismal Study, Heidelberg University, Heidelberg, Germany

[5]Fondazione The Microsoft Research - University of Trento Centre for Computational and Systems Biology, Trento, Italy

[6]BDI, Monash University Clayton VIC, Clayton, Australia

[7]Monash Bioinformatics Platform, Monash University Clayton VIC, Clayton, Australia

[8]Department of Molecular and Cell Biology & Helen Wills Neuroscience Institute, University of California, Berkeley, CA, USA

[9]Department of Physiology, Development and Neuroscience, University of Cambridge, Cambridge, United Kingdom

Correspondence
Lucia Poggi, Molecular and Cellular Ophthalmology Laboratory, Department of Cellular, Computational and Integrative Biology - CIBIO, University of Trento, Via Sommarive, 9, 38123, Trento, Italy.
Email: lucia.poggi@unitn.it

Mirana Ramialison, Australian Regenerative Medicine Institute, Monash University, 15 Innovation Walk Clayton VIC, 3800, Australia.
Email: mirana.ramialison@monash.edu

Present address
Fernando J. Rossello, University of Melbourne Centre for Cancer Research, University of Melbourne, Melbourne, Victoria, Australia
Giuseppina Covello, Department of Biology, University of Padova, Padova, Italy

Abstract

Expression of the bHLH transcription protein Atoh7 is a crucial factor conferring competence to retinal progenitor cells for the development of retinal ganglion cells. Several studies have emerged establishing *ATOH7* as a retinal disease gene. Remarkably, such studies uncovered *ATOH7* variants associated with global eye defects including optic nerve hypoplasia, microphthalmia, retinal vascular disorders, and glaucoma. The complex genetic networks and cellular decisions arising downstream of *atoh7* expression, and how their dysregulation cause development of such disease traits remains unknown. To begin to understand such Atoh7-dependent events in vivo, we performed transcriptome analysis of wild-type and *atoh7* mutant (*lakritz*) zebrafish embryos at the onset of retinal ganglion cell differentiation. We investigated in silico interplays of *atoh7* and other disease-related genes and pathways. By network reconstruction analysis of differentially expressed genes, we identified gene clusters enriched in retinal development, cell cycle, chromatin remodeling, stress response, and Wnt pathways. By weighted gene coexpression network, we identified

coexpression modules affected by the mutation and enriched in retina development genes tightly connected to *atoh7*. We established the groundwork whereby Atoh7-linked cellular and molecular processes can be investigated in the dynamic multi-tissue environment of the developing normal and diseased vertebrate eye.

KEYWORDS

Ath5, human retina, inherited eye diseases, retinal ganglion cells, transcriptome analysis

1 | INTRODUCTION

Retinal ganglion cells (RGCs) collect visual information from the neural retina in the eye and convey it to the visual cortex of the brain. In healthy people, this information is transmitted along the optic nerve, which is composed mainly of axons formed from the cell bodies of RGCs. Inherited diseases affecting the development of RGCs and the optic nerve can interrupt this information flow causing permanent blindness.[1,2] Atoh7 is an evolutionarily conserved, developmentally regulated transcription factor crucial for the genesis of RGCs in different vertebrate models.[3-7] Studies have shown that induced or naturally occurring mutations in the *atoh7* gene result in retinal progenitor cells (RPCs) failing to develop into RGCs and the optic nerve.[3,5,6] Likewise, an increasing number of studies highlight *ATOH7* as an emerging candidate for eye diseases in humans. Variations in the *ATOH7* locus have been associated with optic nerve hypoplasia (ONH) and aplasia (ONA),[8-11] further pointing towards the crucial role of *atoh7* in RGC genesis and optic nerve development. Remarkably, a number of studies have also emerged, which highlight *ATOH7* variants as associated with multiple eye disease traits. These include disorders of the retinal vasculature, such as retinal non-attachment (NCRNA) and persistent hyperplastic primary vitreous (PHPV) (OMIM:# 221900, ORPHA:91495),[8,10,12-17] as well as corneal opacity, microcornea, microphthalmia (ORPHA:289499),[10,18] and glaucoma.[19] The Atoh7-regulated gene networks involved, and how their disruption contribute to the development of such ocular disorders remain unknown.

The zebrafish has long been valued as a paradigm for disentangling the genetics and cell biology of fundamental eye developmental processes.[20,21] The rapidly and externally developing transparent zebrafish embryos are amenable to easy genetic manipulation, allowing fast generation and identification of mutants modelling human ocular genetic disorders.[22-28] Such disease models can be concurrently investigated in large-scale genetics, drug screening, in vivo cell biology of early disease development as well as behavioral assays.[29-32] These potentials substantially aid fast progress in the validation of human genome association studies and in preclinical therapy development paths

toward the early diagnosis and/or restoration of visual function.[33-36]

We here begin to explore the potentials of the *lakritz* zebrafish mutant carrying a loss of function mutation in the *atoh7* gene.[6] With the analysis of available microarray data, we investigate Atoh7-regulated gene networks and interrogate how deregulation of these networks during early onset of RGC genesis might contribute to the development of *atoh7*-associated eye disorders. We provide a cohort of statistically significantly regulated Atoh7 target genes, including previously known Atoh7 targets such as *atoh7* itself.[37,38] Remarkably, at this early RGC developmental time-point, the most significant targets comprehend previously unreported eye field transcription factors, Wnt signaling pathway components, chromatin and cytoskeletal regulators, and even stress-response proteins as major Atoh7-regulated genes. Furthermore, several components of these pathways include eye disease gene markers.

With these data in hand, we can now begin to exploit the power of zebrafish as *in vivo* vertebrate model to assess how dysregulation of one or more of these components might affect the coordinated development of ocular tissues. This will hopefully provide us with a next step forward in the identification of potential targets for the early detection and/or specific treatment of inherited eye diseases such as retinal-vascular disorders.

2 | MATERIALS AND METHODS

2.1 | Wild-type and transgenic zebrafish

Fish used in this study were identified heterozygous carriers of the *lakritz* mutation[6] crossed in the (AB/AB) background as well as transgenic *tg(lakritz/atoh7:gap43-RFP)* heterozygous carriers.[38,39] All fish were maintained at 26°C-28°C as described previously.[40,41] Embryos were obtained by breeding adult male and female fish at ratio 1:1. After fertilization, eggs were collected and maintained at 28.5°C and staged using standard morphological criteria.[40] Fish were kept and experiments were performed in accordance to local animal welfare agencies and European Union animal welfare guidelines.

2.2 | Eyes and body sample collection

Single pairs of eyes were dissected from single embryos at 25, 28, 35, 48, 72, and 96 hpf and snap-frozen in liquid nitrogen, and stored at −80°C. Embryos older than 28 hpf were first anesthetized for 5-10 minutes in ethyl 3-aminobenzoate methanesulfonate (MS-222) (Sigma-Aldrich) in E3 medium. The corresponding body of each embryo was collected and used immediately to perform genotyping analysis to identify the corresponding *lakritz* and wild-type eyes. All embryos were collected from the same batches of fish stock to maintain a uniform genetic background.

2.3 | DNA extraction from zebrafish body biopsies and genotyping

Genomic DNA extraction from each single body was performed in 100 μL of lysis buffer containing Proteinase K-20 mg/mL (EuroClone S.p.A. Milan, Italy), 2 mol/L Tris-HCl ph 8.0, 0.5 mol/L EDTA ph 8.0 and 5 mol/L NaCl, 20% SDS in a final volume of 50 μL ultra H_2O. After 3 hours of incubation at 65°C, the gDNA was purified with an ethanol precipitation step and re-suspended in 50 μL of Dnase/Rnase H_2O. The genotyping was performed by restriction fragment length polymorphism (RFLP) assay as previously described.[6] An ~300 bp fragment of *atoh7* was PCR amplified with 1 U Taq DNA polymerase (Applied Biosystems by Life Technologies, Carlsbad, CA, USA) according to the manufacturer protocols in a 30 μL PCR mix containing 100 ng of purified gDNA (from each single embryo body) with the following primers: Forward 5′-CCGGAATTACATCCCAAGAAC-3′ and Reverse 5′-GGCCATGATGTAGCTCAGAG-3′. The PCR conditions were as follows: initial denaturation (95°C for 5 minutes), followed by 40 cycles of denaturation (95°C for 45 seconds), annealing (56°C for 45 seconds), extension (72°C for 45 second), and a final extension at 72°C for 5 minutes. The resulting PCR product was digested with StuI restriction enzyme (NEB), according to the manufacturer's protocols. The digested product was analyzed on a 2% agarose gel in 1X Tris-Acetate EDTA (TAE) buffer (Sigma-Aldrich) to highlight wild type or *lakritz* mutant corresponding fragments. The L44P mutation[6] eliminates a restriction site found in the L44 allele[42] and therefore can be visualized as an undigested ~300 bp fragment rather than the ~100 and ~200 bp fragments expected from the wild-type condition (Figure 1B). 1Kb DNA Ladder was used as a reference (Gene ruler 1Kb plus, Thermo Scientific).

2.4 | Affymetrix arrays hybridization and analysis

For the microarray analysis, three pairs of wild-type and *lakritz* 28-30 hpf embryos representing three biological replicates
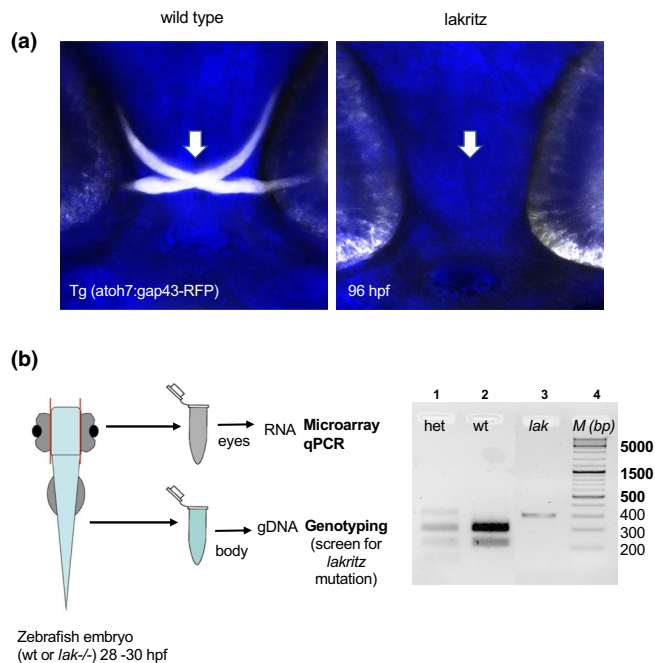

FIGURE 1 Scheme of the experimental design for the comparative array analysis. A, Confocal images showing examples of wild-type and *lak−/−* (*lakritz*); *tg(atoh7:gap43-RFP)* embryos at 96 hpf. The RFP-positive optic chiasm and RGCs are absent in the retina of a *lakritz* embryo. B, Pairs of eyes were dissected from single embryos at 25, 28, 35, 48, 72, and 96 hpf . Genotyping on the gDNA extracted from each corresponding cell body was performed to identify *lakritz* and wild-type embryos (see materials and methods section). The RNA extracted from each pair of eyes corresponding to either a *lakritz* or wild-type embryo was amplified and used for the microarray analysis and qRT-PCR expression analysis. [Color figure can be viewed at wileyonlinelibrary.com]

were dissected and placed in Trizol reagent (Thermo scientific Life Technologies) for the total RNA extraction according to the manufacturer's instructions. T7-based linear amplification of the mRNA was performed using the megascript kit from Ambion. Hybridization was performed on the Affymetrix GeneChip platform and processed according to standard procedure.[43]

Correspondence between Zebrafish Affymetrix probesets and EnsEMBL gene annotations was retrieved using BioMart (EnsEMBL Version 84, March 2016).[44] Batch effect removal was applied to adjust for known batch effect by first filtering the normalized matrix of intensities discarding probes with total abundance between samples lower than first quartile (Q1 = 16.26), and then correcting intensities using ComBat package[45] with extraction day as the known batch (Figure S1). Differential expression analysis between mutant and wild-type samples was performed using Limma package.[46] For probes showing statistically significant differential expression (adj. P value < 0.05), annotations of corresponding genes were retrieved from the EnsEMBL database using BiomaRt package.[47]

TABLE 1 List of primers with amplicon sizes used for quantitative real-time PCR

Primers	Sequence (5′> 3′)	Product length (bp)
GAPHD_zf FOR	TCACAAACGAGGACACAACCA	219
GAPHD_zf REV	CGCCTTCTGCCTTAACCTCA	
Ube2a_zf FOR	CTGAAGGAACACCTTTTGAAGATG	215
Ube2a_zf REV	GATCCAGTAAAGACTGTATTGAG	
Atoh7_zf FOR	TCACCTGTGGAAAGTGACTG	254
Atoh7_zf REV	CTCATTCACAACCCGCCCAA	
Anln_zf FOR	AAAGGCTTCCTGACTATGTTTG	107
Anln_zf REV	CATCATCAGGGTAGGTCCA	

2.5 | Quantitative Real-Time PCR (qRT-PCR)

For the qRT-PCR analysis of *anillin* and *atoh7*, total RNA from five pulled pairs of frozen eyes, corresponding to either *lakritz* or wildtype embryos, was used. After Turbo DNase treatment (Thermo scientific-Ambion), according to the manufacturer instructions, the RNA concentrations were measured with a Nanodrop ND-1000 spectrophotometer (NanoDrop Technologies Inc). The RNA integrity was verified by loading the samples on 1% agarose gel that was run at 100 Volts in TBE 1X. 500 ng of extracted RNA from each sample was retrotranscribed with a RevertAidTM First Strand cDNA Synthesis Kit (Thermo SCIENTIFIC), following the manufacturer's protocol. Quantitative real-time PCR reactions were performed on a Bio-Rad CFX96 Termo-cycler with Kapa Syber Fast qPCR master mix (2×) kit (Sigma-Aldrich), according to the manufacturer's instructions. Templates were 1:10 diluted cDNA samples. For the negative controls, cDNAs were replaced by DEPC water. All real-time assays were carried out using 10 ng of cDNA. The PCR profile was as follows: 15 seconds at 95°C, followed by 40 cycles 60°C for 20 seconds, 72°C for 40 seconds. For the melting curve, 0.5°C was increased every 5 seconds from 65°C to 95°C. All reactions were run in triplicate and both glyceraldehyde-3-phosphate dehydrogenase (GAPDH) and Ubiquitin Conjugating Enzyme E2A (UBE2A) were used as reference genes. Each experiment was performed in triplicate and repeated two times. The relative gene expression was calculated using the $\Delta\Delta$CT method. Statistical analyses were performed with Prism 5 (GraphPad Software), and statistical significance was set to $P < .05$ for all experiments. The values are expressed as mean $\pm$ SEM, and the differences between groups were investigated using unpaired two-tailed Student's *t* test (GraphPad Software). A list of primers is shown in Table 1.

2.6 | Functional category enrichment analysis and network analysis

Functional enrichment analysis was performed with Metascape[48] using the *Danio rerio* EnsEMBL IDs of the list of differentially regulated genes as "Input as species" and "Analysis as species" species through the custom analysis mode. Enrichment analysis was performed against GO "Biological Process" using P value cut-off of < 0.05 and otherwise default parameters. Human disease annotation was performed with Metascape using *Danio rerio* as "Input as species" and *H sapiens* as "Analysis as species." Under the "Annotation" mode, all repositories under Genotype/Phenotype/Disease were selected for disease annotation. To rule out potential sampling or biological bias, we performed an additional enrichment analysis by restricting the background to the list of expressed genes as detected by the arrays, using both Metascape and KOBAS.[49] Network interactions between the differentially expressed genes were retrieved through the STRING database,[50] "multiple proteins" mode and default parameters otherwise. Network interactions were visualized using Cytoscape.[51]

2.7 | Weighted gene co-expression network analysis

The pipeline proposed by Langfelder and collaborators[52] in their CRAN package was followed to infer gene co-expression networks and identify network modules within R 3.6.3 statistical environment. Networks were inferred using the TOMsimilarityFromExpr function with "cor" as gene coexpression measure. The soft-threshold parameter was optimized with the function pickSoftThreshold and the best threshold ($\alpha = 16$) selected by visual inspection to follow a scale-free topology model, as suggested by the WGCNA pipeline. Correlations between modules eigengenes, status, and library batch were computed. Modules with the highest correlation for status and significant P value ($\alpha \leq 0.05$) were selected for further analysis. Within the selected modules, highly connected structure of submodules were identified using the leading eigenvector community detection method[53] implemented in the igraph package (v1.2.5) for R (http://igraph.com).

2.8 | Whole mount immunohistochemistry

For immunohistochemical labelling, embryos were fixed in 4% PFA for 1 hour at room temperature or overnight at 4°C. Embryos were washed three times in PTw and kept for a week maximum in PTw. Fixed embryos were blocked in blocking solution (10% goat serum, 1% bovine serum albumin, and 0.2% Triton X-100 in PBS) for 1 hour. Embryos were permeabilized with 0.25% trypsin-EDTA (1X, Phenol red, Gibco; Life Technologies) on ice for 5 minutes. Primary (mouse anti-β-catenin, 1:100, Cat. No 610153, BD Biosciences) and secondary (anti-mouse IgG conjugated to Alexa Fluor 488, 1:250, Life Technologies) antibodies were added for two overnights each and DAPI was added from the first day of incubation in the antibody mix. Stained embryos were kept in PTw at 4°C in dark until imaging. Embryos were embedded onto a 35 mm Glass-bottom Microwell dish (p35G-1.5-10-C, MatTek) and oriented with a femtoloader tip (Eppendorf, Leipzig, Germany) in the position needed for imaging until the agarose had polymerized. Confocal imaging was performed using a laser scanning confocal microscope Leica SpE using a Leica 40×, 1.15 NA oil-immersion objective.

For the analysis of the intensity along the apical-to-basal membrane, a line of a defined length along the apical-to-basal membrane was drawn for nine cells at three different confocal z-sections for each embryo. Signal intensities were obtained using Fiji[54] and average values for the nine cells were calculated. For the analysis of the intensity along the apical membrane, the number of peaks were counted after Ctnnb1 signal intensity measurement. For the signal intensity measurements, a line of defined length was drawn along the apical membrane of the retina on Fiji[54] and signal intensities were retrieved. The length of line was the same for all z-sections of an individual embryo. Normalization was performed by the highest value for each line. Measurements were obtained on three different Z sections for each embryo.

3 | RESULTS

3.1 | Transcriptome analysis of wild-type and *lakritz* identified 137 statistically significant differentially expressed genes

Expression of *atoh7* in the retina is first detected at around 25-28 hpf and it reaches its peak at around 36 hpf.[42] The earliest post-mitotic RGCs in the retina are detected at around 28 hpf, a developmental time-point corresponding to the earliest onset of retinal differentiation.[55] To identify early Atoh7-regulated genes, transcriptome analysis was performed on eyes from single *lak*^{−/−} mutant (*lakritz*)[6] and wild-type zebrafish embryos at 28-30 hours post-fertilization

(hpf) based on Affymetrix microarrays (see methods and Figure 1).

Differential gene expression analysis performed with LIMMA resulted, after batch effect removal, with 171 significantly differentially expressed probes (adj. *P* value < .05) (Figure 2A) corresponding to 137 genes annotated onto EnsEMBL database (Figure 2B and Table S1). Among these, we confirmed downregulation of *atoh7* in the *lakritz*, consistent with its known role as self-activator.[37] Also consistent with the presence of *bona fide* Atoh7-regulated targets in the 137 cohort is the presence of additional seven genes, which have been previously reported to contain a well-characterized Ath5 consensus binding site.[37,38] Among the eight Atoh7-direct targets, besides *atoh7* itself, the thyrotroph embryonic factor *tefa*[56] and the atypical cadherin receptor 1 *celsr1a* (*CELSR1*)[57] were downregulated in the *lakritz*, suggesting their positive regulation by Atoh7. Conversely, the retina and anterior neural fold homeobox transcription factor *rx1* (*RAX*),[58] the Wnt signaling pathway regulator *notum*,[59] the transmembrane protein *tmem165*,[60] and the F-actin binding protein and cytokinesis regulator *anillin* (*ANLN*)[61] were upregulated in the *lakritz*, suggesting that they are negatively modulated by Atoh7.

3.2 | Functional category enrichment reveals neural retina, cell cycle and Wnt pathways regulated downstream of Atoh7

Functional enrichment analysis in Metascape using default parameters reveals "neural retina development" (GO:0003407) as the most highly significantly enriched GO Biological Process category, consistent with the role of Atoh7 as regulator of retinal development (Figure 3 and Table S2). To further increase stringency, ruling out sampling or biological bias in the analysis, the background was restricted to the list of expressed genes as detected by the arrays[49] using both Metascape and Kobas 3.0, which incorporates knowledge from five pathway databases (KEGG PATHWAY, PID, BioCyc, Reactome, and Panther) and five human disease databases (OMIM, KEGG DISEASE, FunDO, GAD, and NHGRI GWAS Catalog). This analysis consistently underscored "neural retina development" (GO:0 003 407) as the enriched term both by Metascape (not shown) and Kobas (Table S3). This category contains nine statistically significantly differentially expressed genes (including *atoh7*), which comprehend early expressed eye-field transcription factors (EFTFs, *rx1*, and *six6a*),[62-65] stress response and extracellular matrix remodeling factors (*hsp70.1*, *mmp14a*),[66-69] chromatin regulators (*smarca5*)[70] as well as microtubules organizers and cell cycle regulatory proteins (*tubgcp4*, *znf503*, and *gnl2*)[71-73] (Table 2). Other (albeit less significant) relevant biological processes emerging from this analysis were
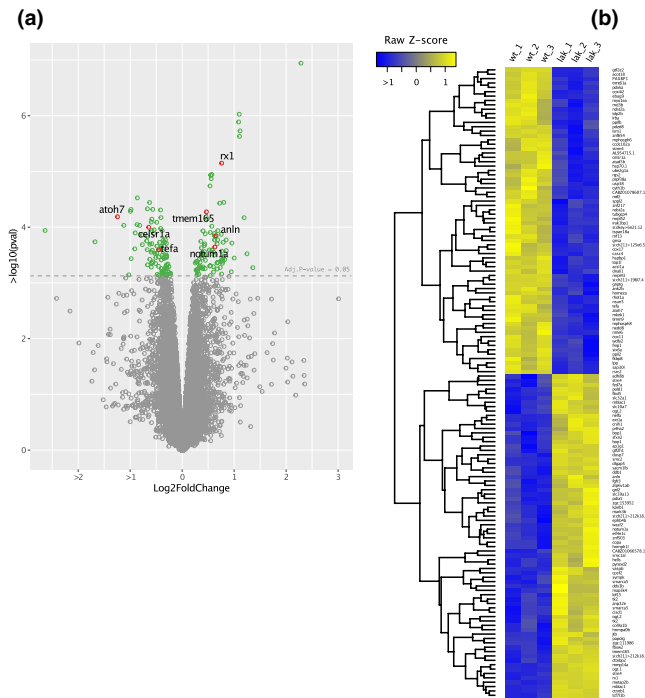
(a)

FIGURE 2 Volcano and heatmap of differentially expressed genes in *lakritz* vs wild-type eyes A,Volcano plot highlighting Atoh7 and its direct targets (in red) among all differentially expressed probes (in green) with adjusted *P* value < 0.05. B, Heatmap was constructed by calculating row Z-score using normalized log2 intensities of 144 of the 171 differentially expressed probes with corresponding gene annotation, using complete hierarchical clustering in R. [Color figure can be viewed at wileyonlinelibrary.com]
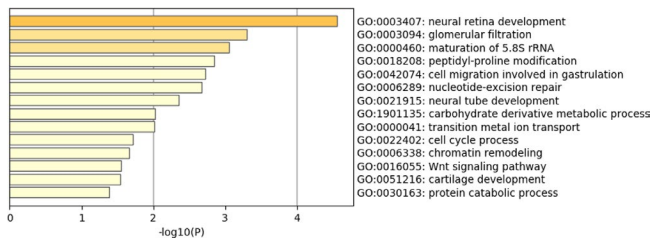

FIGURE 3 Functional enrichment analysis. Statistically significantly over-represented GO Biological Process categories (Metascape). See also Table S2 [Color figure can be viewed at wileyonlinelibrary.com]

"cell cycle process" (GO:0022402), "chromatin remodeling" (GO:0006338), and "Wnt signaling pathway" (GO:0016055) (Figure 3 and Table S2).

We next investigated the known relationships among the 137 Atoh7-regulated genes via network reconstruction analysis (see methods). Interestingly, analysis conducted with STRING-DB v 11.0 highlighted *atoh7*, *rx1*, and *six6a* as the core of a retinal "kernel" composed of early developmental eye-specific transcription factors[74] (Figure 4). Furthermore, this analysis highlighted three main gene subnetworks, which are suggestive of the over-represented GO Biological

processes, namely "retinal development," "cell cycle/chromatin remodeling," and "Wnt signaling pathway" (Figure 4).

Among the *bona fide* genes integrating into the "cell cycle/chromatin remodeling" subnetwork is the F-actin binding and cytokinesis regulator Anillin (*ANLN*[38,75,76]). Studies in the zebrafish retina have shown that *anillin* expression levels are required to favor cell cycle progression and restrict RGC genesis in Atoh7-expressing RPCs.[38] Concordantly, in the presence of *anillin* downregulation, many more RPCs turn on *atoh7* and become RGCs,[38] In agreement with these findings, our results show that *anillin* is an Atoh7-downregulated gene (Figure 2). Studies have reported *anillin* expression positively associated with the expression of β-catenin (*ctnnb1*).[77] Interestingly, our results indicate that *ctnnb1* is an Atoh7-downregulated gene as well as a central gene of the "Wnt signaling pathway" emerging in the network reconstruction analysis (Figure 4). Given the reported role for Wnt/β-catenin signaling in retinal development and regeneration,[77] we sought to uncover possible interplay between Anillin and β-catenin in the developing zebrafish retina. In support of this hypothesis, we find that *anillin* knockdown[37] causes accumulation and displacement of the β-catenin signal in the apical and apical-lateral membrane of RPCs at 30 hpf (Figure 5A,B). Further studies linked *anillin* to angiogenesis and retinal neovascularization processes, leading to the obvious hypothesis that *anillin* regulation is relevant for retinal vascular development.[79] If this were the case, we should find *anillin* expression being regulated beyond the RGC differentiation period. To begin to assess this possibility, we carried out quantitative real-time RT-PCR (qRT-PCR) analysis of *anillin* starting from 25 hpf until after 72 hpf, when all retinal cells are fully differentiated in the central zebrafish retina.[55] Interestingly, *anillin* expression levels remain significantly upregulated by the *lakritz* condition (Figure 5C) even at 72 hpf. Furthermore, the trend of *anillin* upregulation in subsequent developmental stages suggests oscillatory dynamics of *anillin* regulation during eye development (Figure 5C).

3.3 | Weighted Gene Co-expression Network Analysis revealed a coexpression module with a cluster of genes tightly interconnected to Atoh7

To explore global changes of gene expression in the *lakritz* mutant, a weight gene co-expression network analysis (WGCNA)[52] was performed. Notwithstanding the small number of array samples, we identified 16 recurrent functional modules based on co-expression pattern analysis on the full transcriptome dataset. To identify co-expression modules significantly affected by the *lakritz* mutation, we tested their association with available covariates, including batch and mutation status. Out of the 16 modules found, two of them showed a high correlation with the mutation condition

TABLE 2 Significantly differentially expressed genes belonging to the "neural retina development" category (see also Figure 3 and Table S2)

GO:0003407 neural retina development

| Input ID	Gene Symbol	H Gene ID	Synonyms	Orphanet	OMIM
ENSDARG00000005374	tubgcp4	**TUBGCP4**	76P|GCP-4|GCP4|Grip76|MCCRP3	[2518] Autosomal recessive chorioretinopathy-microcephaly	OMIM:609610
ENSDARG00000098080	gnl2	**GNL2**	HUMAUANTIG|NGP1|Ngp-1|Nog2|Nug2		OMIM 609365
ENSDARG00000052348	smarca5	**SMARCA5**	ISWI|SNF2H|WCRF135|hISWI|hSNF2H	[370334] Extraskeletal Ewing sarcoma	OMIM:603375
ENSDARG00000002235	mmp14a	**MMP14**	MMP-14|MMP-X1|MT-MMP|MT-MMP 1|MT1-MMP|MT1MMP|MTMMP1|WNCHRS	[85196] Nodulosis-arthropathy-osteolysis syndrome;[3460] TORG-WINCHESTER SYNDROME	OMIM:600754
ENSDARG00000018492	znf503	**ZNF503**	NOLZ-1|NOLZ1|Nlz2		OMIM:613902
ENSDARG00000025187	six6a	**SIX6**	MCOPCT2|ODRMD|OPTX2|Six9	[264200] 14q22q23 microdeletion syndrome;[435930] Colobomatous optic disc-macular atrophy-chorioretinopathy syndrome;[2542] Isolated anophthalmia-microphthalmia	OMIM:606 326
ENSDARG00000029688	hsp70.1	**HSPA1L**	HSP70-1L|HSP70-HOM|HSP70T|hum70t		OMIM:140559
ENSDARG00000069552	atoh7	**ATOH7**	Math5|NCRNA|PHPVAR|RNANCL|bHLHa13	[289499] Congenital cataract microcornea with corneal opacity;[91495] Persistent hyperplastic primary vitreous	OMIM:609 875
ENSDARG00000071684	rx1	**RAX**	RX |MCOP3	[2542] Isolated microphthalmia-anophthalmia-coloboma	OMIM:601881
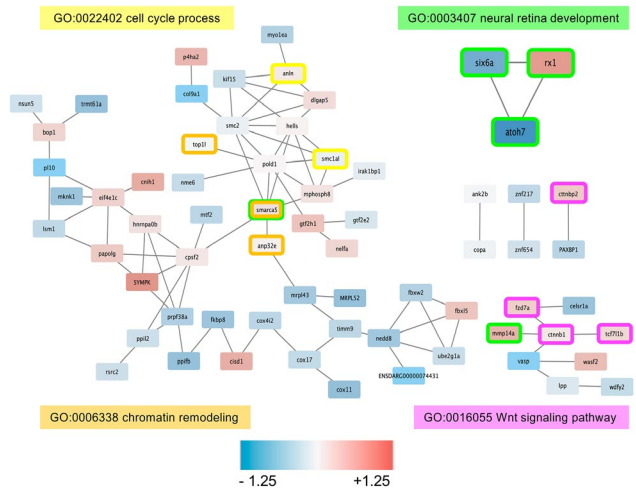
FIGURE 4 Interaction network downstream of Atoh7. Known interactions between downstream targets of Atoh7 from the STRING database visualized with Cytoscape (genes without known interactions are not represented). Node colours represent the log2 fold-change of gene expression in *lakritz* vs wild-type eyes. Node borders are coloured by gene ontology annotation: "neural retina development" (green), "cell cycle process" (yellow), "Wnt signaling pathway" (pink), and "chromatin remodeling" (orange) [Color figure can be viewed at wileyonlinelibrary.com]

FIGURE 5 Dysregulation of Ctnnb1 localization by *anillin* knockdown and *anillin* expression dynamics. A, Ctnnb1 staining in control (ctrlMO, n = 3 embryos) versus *anillin* knockdown (anlnMO, n = 3 embryos) in morpholino injected embryos at 30hpf. Arrows show apical location, arrowheads show apical-to-basal location. B, Graph showing the normalized Ctnnb1 intensity signal along the basal-to-apical membrane of the apical-most cells in control (n = 3 embryos) versus anlnMO (n = 3 embryos) injected embryos. The colored line shows the averaged intensity of all lines for the ctrlMO and anlnMO. Boxplot showing the number of peaks of Ctnnb1 signal intensity along the apical surface in ctrlMO (n = 3 embryos) versus anlnMO (n = 3 embryos) injected embryos. $P < 10^{-4}$. Center lines show the medians; crosses show the means; box limits indicate the 25th and 75th percentiles as determined by R software; whiskers extend 1.5 times the interquartile range from the 25th and 75th percentiles, data points are represented as circles. Student's *t* test. C, *Anillin* mRNA levels show dynamic variations during subsequent developmental stages. qRT-PCR was performed on eyes from *lakritz* or wild-type embryos at 25, 35, 48, 72 (left) and 96 hpf (right) to assess the trend of *anillin* and *atoh7* expression. The relative gene expression (*lakritz* vs wild type) was calculated using the CT method for each stage. Histogram values are expressed as mean ± SEM. ($P < .05$) and the mRNA levels of both *gapdh* and *ube2a* were used as internal controls. The statistical analysis is described in the methods section. [Color figure can be viewed at wileyonlinelibrary.com]

(wild type vs *lakritz*). Specifically, modules 13 (overall up-regulated) and module 3 (overall downregulated) were found highly significant with a correlation of 0.97 ($P = .002$) and -0.99 ($P = $ 1e-5), respectively (Figure S2 and Table S4). Functional network analysis by STRING DB https://www.string-db.org/) on M13 - the smallest module, which we also found to contain *atoh7* - revealed an enrichment in "eye morphogenesis (blue color in Figure S3), "retina layer formation" (red color in Figure S3), and a cluster of genes previously found to be dysregulated in "light responsive, circadian rhythm processes" (PMID: 20830285 and PMID: 21390203) (light and dark green color in Figure S3).

Lastly, we analyzed in detail the topology of the Module 13. We identified four submodules with high within-community connectivity, which show decreasing degree of connectivity from left to right (Figure 6). The submodule containing *atoh7* (left) shows a densely interconnected cluster of genes with high topological overlap. These genes likely participate in common regulatory and signaling circuits including retina layer formation (eg, *atoh7*, *rx1*) and Wnt/β-catenin signaling pathway (eg, *fxd7a, tcf7l1b*).

4 | DISCUSSION

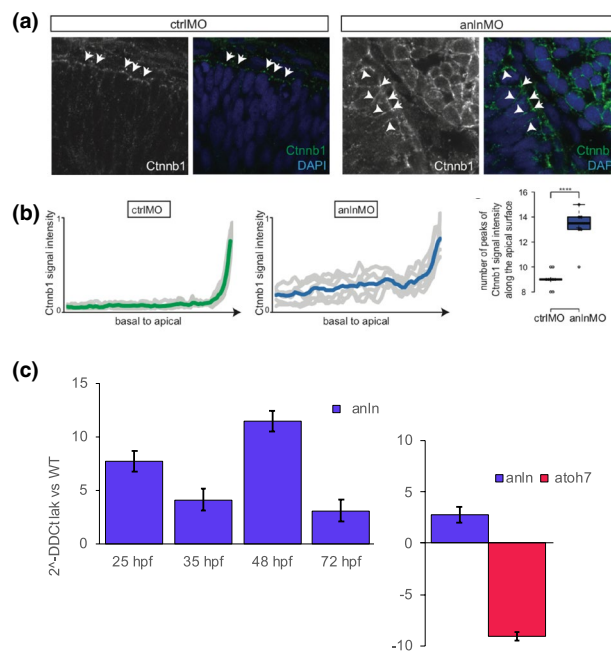Our differential gene expression analysis of transcriptome data revealed 137 genes that are significantly differentially expressed between *lakritz* and wild-type eyes from embryos at a developmental time-point corresponding to the onset of RGC differentiation. We also applied multiple bioinformatics pipelines to perform a functional classification and network reconstruction of the differentially expressed genes. Notably, all methods here applied consistently highlighted "neural retina development" (GO:0003407) as the most biological pathway differentially affected by the *lakritz* mutation. Likewise,

the interplay *atoh7*, *rx1*, and *six6a*—early developmentally regulated EFTs—consistently emerged as the "kernel" network of this cluster

The homeobox transcription factor Rx1 is well known for its evolutionarily conserved role in the generation and maintenance of multipotent RPCs during morphogenesis and differentiation of the vertebrate eye.[63,65,80-83] Mutant variants of *RAX* family genes have been linked to congenital developmental eye disorders, particularly microphthalmia, further confirming an early requirement for RPC proliferation and stemness.[17,84-86] Based on these findings, the data from our analysis suggest that balancing RPCs competence and RGC fate commitment requires *rx1* downregulation by Atoh7. Notably, Atoh7-mediated downregulation of *rx1* is likely direct, since previous in silico analyses highlighted the presence of an Atoh7-binding motive in the *rx1* gene cis-regulatory regions.[37]

Conversely, *six6* genes have been reported as RPCs competence factors, on the one hand suppressing stemness and proliferation via Wnt/β-catenin signaling downregulation, on the other hand promoting expression of RGC differentiation genes.[62] These findings are in agreement with the present study reporting *six6a* being an Atoh7-upregulated gene. Remarkably, variant forms of *SIX6* (*SIX9/OPTX2*) have been linked to congenital microphthalmia as well as to the development of glaucoma.[17,87-94] Given that mutations in *ATOH7* have been also associated with similar global eye disorders,[10,95] these observations strongly point at the importance to further our understanding of the interplay *ATOH7*, *RX1*, and *SIX6* during eye development as well as to assess how disruption of this evolutionarily conserved genetic network might be linked to such eye disorders.[96]
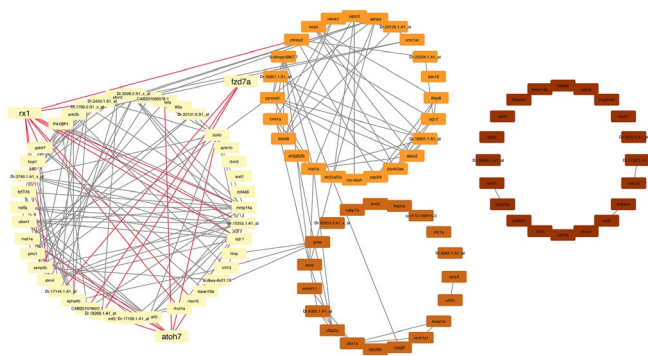

FIGURE 6 Detailed topology of Module 13. Each node represents a gene while a connection represents a co-expression between two genes (only the first 200 edges in order of co-expression weight were retained for visualization purposes). Submodules are shown with decreasing degree of connectivity from left to right. Highlighted edges represent the connection between retina layer formation and Wnt-related genes [Color figure can be viewed at wileyonlinelibrary.com]

Besides *atoh7*, *rx1*, and *six6a*, significant differentially expressed genes annotated with "neural retina development" were *tubgcp4*, *gnl2*, *smarca5*, *mmp14a*, *znf503*, and *hsp70.1*. The Atoh7-upregulated gamma-tubulin complex protein 4 encoding gene *tubgcp4* is of great interest. Variants of *TUBGCP4* have been linked to autosomal-recessive microcephaly with chorioretinopathy, which comprise a spectrum of eye developmental anomalies including microphthalmia, optic nerve hypoplasia, retinal folds, and absence of retinal vasculature.[71] This raises the possibility that regulation of this gene might link Atoh7 to retinal-vascular development as well as retinal neurogenesis. Genetic evidences for the GTPase and zinc finger transcriptional repressor encoding genes, *gnl2* and *znf503* (*NOLZ1*) as eye disorders-related genes are still missing but studies support their functional requirement for retinal developmental processes, including proper cell cycle exit of RPCs during RGC differentiation.[72,73] Notably, *tubgcp4*, *gnl2* and *znf503* were implicated in the regulation of cytokinesis late in mitosis.[71-73] This observation further indicates Atoh7 requirements for the regulation of cell cycle progression, at least in RPCs. The SWI/SNF chromatin remodeling factors have been reported as crucial regulators of the transition from multipotent to committed progenitor and differentiated cell states in multiple eye tissues, with potential implications for eye disorders.[97-100] The finding of *smarca5* as an upregulated gene in the *lakritz* indicates the importance to address functional implications of this chromatin remodeling gene for *atoh7*-related eye disorders. Furthermore, the "neural retina development" Gene Ontology category encompassed the reportedly stress response genes *hsp70.1(HSPA1L)*[69] and *mmp14*[101] as significantly downregulated and upregulated, respectively, by the *lakritz* mutation. The crystallin related, heat shock Hsp70 family proteins are emerging as important regulators of RGC survival and regeneration as well as retinal vascular remodeling factors.[69,102-104] The intriguing finding that *hsp70.1* is highly enriched among the Atoh7-upregulated genes in the "neural retina development" gene cluster supports the idea that upregulation of these stress-response proteins might be relevant also during RGC development. Lastly, the extracellular matrix remodeling factor Mmp14 is reportedly a crucial regulator of cell stemness and vascular remodeling.[105] Studies have also implicated Mmp14a in retinal developmental processes such as RGC axon guidance and innervation of the optic tectum.[66-68] Future studies will assess the functional implication of Atoh7-mediated downregulation of *mmp14a* during vascular-retinal development. Interestingly, our network analysis reveals that *mmp14a* is linked with known components of the Wnt signaling pathway, further underscoring the importance of the interplay of this pathway and Atoh7.

The "Wnt signaling pathway" is the second Atoh7-dependent subnetwork emerging in our functional network analysis, which is centered around the *ctnnb1* (β-catenin)

gene (Figure 4). Studies have shown that the Wnt/β-catenin pathway promotes RPC proliferation and stemness while suppressing *atoh7* activation and RGC differentiation.[106-108] We here find that the main differentially expressed components of this pathway, namely *ctnnb1*, *fxd7a*, and *tcf7l1b*, are up-regulated in the *lakritz* mutant, suggesting Atoh7 requirement in the Wnt/β-catenin pathway downregulation (Figure 4). Concordantly, studies have reported that *atoh7*-expressing RPCs contain low levels of expression in Wnt/β-catenin pathway components when compared with non-*atoh7*-RPCs.[109] This further suggestive of a negative feedback regulatory loop integrating Atoh7 and Wnt/β-catenin signaling. Conversely, the planar cell polarity (PCP) signaling component *celsr1a/flamingo*, which has been reported as key regulator of neuronal cell differentiation, neurite outgrowth, and axon guidance,[110] emerges as an Atoh7-upregulated gene in our cohort. A number of studies reported dysregulation of Wnt signaling being associated with retinal diseases.[108,111-113] Likewise, Wnt, Fzd7/β-catenin pathway has been reported as an important modulator of retinal vascular remodeling.[114] Further research will clarify the genetic regulatory networks integrating Atoh7 and Wnt/β-catenin signaling in controlling multiple eye tissue development in the vertebrate, and how their dysregulation might results in multiple ocular disorders.[115]

Previous studies highlighted the importance of the interplay of Atoh7 with components of the Notch signaling pathway for RGC development and regeneration.[116-118] In particular, downregulation of Notch signaling pathway has been proposed as a general mechanism whereby RGC genesis can be enhanced.[116,119-121] In agreement with these findings, Notch pathway components (*hes6*, *mib1*, *hdac*, *adam17b*, and *Notch1a*) appear affected by the *lakritz* mutation in our gene expression microarray data but their expression does not change significantly between wild-type and *lakritz* condition in our analysis (Table S1). However, even though they fail short of the significance threshold of adjusted *P* value < .05, it is worth noting that their values suggest a trend in downregulation of Notch pathway-related genes (Table S1). We suppose that such lack of significance in the differential expression might be linked to the developmental stage used for this analysis. Likewise, the extracted cohort of significantly regulated genes does not comprehend some of the reported RGC maturation-associated factors, such as Cxcr4b, Elavl3, and Isl1.[37,38,109,122] Nonetheless, for *cxcr4b* and *elavl3a*, −1.43 FC (nominal *P* value of .0018) and −1.39 FC (nominal *P* value .0066) was observed, respectively, consistently with a positive regulation by Atoh7 (downregulated in the *lakritz*). We therefore suppose that expression of such RGC maturation-related factors downstream of Atoh7 might be too low at the developmental time-point selected for this study, to be detected within the chosen significance range. In support of the Atoh7-dependent transcriptional regulation of RPC

division and developmental progression, a third Atoh7-dependent subnetwork emerged in our functional network analyses, which includes cell-cycle and chromatin regulators (Figure 4). One *bona fide* gene of great interest in this subnetwork is the F-actin binding and cytokinesis regulator Anillin (*ANLN*).[38,75,76] Anillin has attracted increasing attention as a potential disease-related gene (ORPH:93213, OMIM:616027). Evidence point at *anillin* expression levels being associated with cell proliferation and migration disorders in cancer and kidney diseases.[123-126] Additional roles for this actin binding protein have been reported in nerve cell development[127,128] and dysregulation of Anillin has been implicated in central nervous system myelin disorders.[129] We here find *anillin* as an Atoh7-downregulated gene. This is in line with earlier observations supporting the suggestion of a molecular feedback regulatory loop of an as yet unknown nature between *anillin* and *atoh7* balancing RPCs developmental progression.[38] While further investigations will address this question, the functional and network analyses from this study suggest that the Wnt/β-catenin signaling might be involved. We indeed made preliminary observations indicating that *anillin* is required for the accumulation and/or localization of β-catenin in the apical and apical-lateral membrane of RPCs. Notably, in addition to promoting cell-to-cell adhesion[130,131] β-catenin functions as nuclear transcriptional co-activator of Wnt signaling responsive genes promoting proliferation and inhibiting differentiation.[78,132,133] Thus, regulation of β-catenin accumulation and localization to the E-Cadherin/β-catenin complex might be a mechanism whereby Anillin controls not only cell adhesion dynamics but also Wnt signaling pathway activity.[130] It was also intriguing to note that *anillin* expression levels are affected by the *lakritz* mutation even after neurogenesis is completed in most of the central retina of the zebrafish eye.[55] Given that Anillin has been reported as potential regulator of choroidal angiogenesis,[79,134] it is tempting to speculate that both RPCs and endothelial cell behaviors require *anillin* expression levels during retinal-vascular developmental interactions. Future studies will assess the functional implications of the interplay of Atoh7, RGC genesis, Anillin and Wnt pathway components for the dysregulation of developmental vascular-retinal disorders.

Finally, we have applied weighted gene co-expression network analysis to explore gene co-expression relationships and identify co-expression modules potentially involved in *atoh7* function. In addition to highlighting the already known interaction networks that were enriched within the 137 differentially regulated genes, we were able to identify two co-expression modules significantly affected by the *lakritz* mutation (Table S4). One of them in particular (module 13) contains a cluster of highly interconnected genes including *atoh7* itself, *rx1* and members of the

Wnt signaling pathway (eg, *tcf7l1b*, *fzd7a* and *mmp14a).* This analysis therefore further confirms tight functional interaction between neural retinal development and Wnt pathway genes from our gene differential expression data. Lastly, our knowledge-based analysis of the M13 members by STRING database further extended these finding by revealing the existence of a network of interactions between *atoh7*- and *rx1*-dependent "retina layer formation," "eye morphogenesis" pathways, Wnt signaling pathway components (eg, *tcf7l1b*, *fzd7a*, and *mmp14a),* and two new gene networks previously found to be dysregulated in light responsive, circadian rhythm processes[56,135] (Figure S3). At present, very little is known on the functional importance of circadian clock genes, but increasing evidence indicates their implication in multiple eye tissues developmental processes as well as ocular disorders.[136-140] This study further supports this evidence, by showing that Atoh7-dependent regulatory networks integrates such circadian clock genes.

In sum, this Atoh7 targets analysis extends data from other studies focusing on transcription factors cascades enhancing RGC differentiation. We here provide new insights on Atoh7-dependent developmental processes that might be regulated in global developmental eye disorders. First, they suggest that Atoh7 directly controls a two-tiered regulatory network balancing early acquisition of progenitor cell competence (eg, through *six6a*, *rx1*) and repression of pro-multipotency and proliferative processes (eg, through chromatin remodeling, cell cycle, and Wnt pathway regulation). Second, these data highlight for the first time many previously unreported cytoskeletal proteins, chromatin remodeling factors, stress-response proteins, and even circadian clock genes as Atoh7-regulated genes. Third, this analysis underscores both direct and potential functional genetic links of many of these factors to eye developmental disorders. This study thus contributes to laying the groundwork for the identification of key candidate molecules and their networks as potential targets for early eye disease detection and therapeutic applications.

AUTHORS' CONTRIBUTIONS
L. Poggi designed research; G. Covello, A-L Duchemin, FB Tremonti, L. Poggi and J. Ngai performed experiments; FJ Rossello, M. Filosi, F. Gajardo, E. Domenici, M. Eichenlaub, M. Ramialison performed bioinformatic analysis with inputs from JM Polo, D. Powell, M. L. Allende; L. Poggi and M. Ramialison wrote the manuscript with inputs from all authors.

DATA AVAILABILITY STATEMENT
The microarray raw intensity data and the related code used to process and analyse the data are freely and publicly available on: https://github.com/fgajardoe/Lakritz_zebra fish_DE_analysis

REFERENCES
1. Dutton GN. Congenital disorders of the optic nerve: excavations and hypoplasia. *Eye*. 2004;18:1038-1048.
2. Zeki SM, Dutton GN. Optic nerve hypoplasia in children. *Br J Ophthalmol*. 1990;74(5):300-304.
3. Brown NL, Patel S, Brzezinski J, Glaser T. Math5 is required for retinal ganglion cell and optic nerve formation. *Development*. 2001;128:2497-2508.
4. Kanekar S, Perron M, Dorsky R, et al. Xath5 participates in a network of bHLH genes in the developing xenopus retina. *Neuron*. 1997;19:981-994.
5. Wang SW, Kim BS, Ding K, et al. Requirement for math5 in the development of retinal ganglion cells. *Genes Dev*. 2001;15:24-29.
6. Kay JN, Finger-Baier KC, Roeser T, Staub W, Baier H. Retinal ganglion cell genesis requires lakritz, a zebrafish atonal homolog. *Neuron*. 2001;30:725-736.
7. Sapkota D, Wu F, Mu X. Focus on molecules: Math5 and retinal ganglion cells. *Exp Eye Res*. 2011;93:796-797.
8. Brown NL, Dagenais SL, Chen CM, Glaser T. Molecular characterization and mapping of ATOH7, a human atonal homolog with a predicted role in retinal ganglion cell development. *Mamm Genome*. 2002;13:95-101.
9. Atac D, Koller S, Hanson JVM, et al. Atonal homolog 7 (ATOH7) loss-of-function mutations in predominant bilateral optic nerve hypoplasia. *Hum Mol Genet*. 2020;29:132-148.
10. Khan K, Logan CV, Mckibbin M, et al. Next generation sequencing identifies mutations in atonal homolog 7 (ATOH7) in families with global eye developmental defects. *Hum Mol Genet*. 2012;21:776-783.
11. Lim S-H, Germain ES, Tran-Viet K-N, et al. Sequencing analysis of the ATOH7 gene in individuals with optic nerve hypoplasia. *Ophthalmic Genet*. 2014;35:1-6.
12. Garcia-Montalvo IA, Pelcastre-Luna E, Nelson-Mora J, Buentello-Volante B, Miranda-Duarte A, Zenteno JC. Mutational

screening of FOXE3, GDF3, ATOH7, and ALDH1A3 in congenital ocular malformations. Possible contribution of the FOXE3 p.VAL201MET Variant to the risk of severe eye malformations. *Ophthalmic Genet*. 2014;35:190-192.

13. Ghiasvand NM, Rudolph DD, Mashayekhi M, Brzezinski JA, Goldman D, Glaser T. Deletion of a remote enhancer near ATOH7 disrupts retinal neurogenesis, causing NCRNA disease. *Nat Neurosci*. 2011;14:578-588.

14. Khor CC, Ramdas WD, Vithana EN, et al. Genome-wide association studies in Asians confirm the involvement of ATOH7 and TGFBR3, and further identify CARD10 as a novel locus influencing optic discarea. *Hum Mol Genet*. 2011;20:1864-1872.

15. Kondo H, Matsushita I, Tahira T, Uchio E, Kusaka S. Mutations in ATOH7 gene in patients with nonsyndromic congenital retinal nonattachment and familial exudative vitreoretinopathy. *Ophthalmic Genet*. 2016;37:462-464.

16. Prasov L, Masud T, Khaliq S, et al. ATOH7 mutations cause autosomal recessive persistent hyperplasia of the primary vitreous. *Hum Mol Genet*. 2012;21:3681-3694.

17. Wright CF, Fitzgerald TW, Jones WD, et al. Genetic diagnosis of developmental disorders in the DDD study: a scalable analysis of genome-wide research data. *Lancet*. 2015;385:1305-1314.

18. Khan K, Al-Maskari A, McKibbin M, et al. Genetic heterogeneity for recessively inherited congenital cataract microcornea with corneal opacity. *Investig Ophthalmol Vis Sci*. 2011;52:4294-4299.

19. Venturini C, Nag A, Hysi PG, et al. Clarifying the role of ATOH7 in glaucoma endophenotypes. *Br J Ophthalmol*. 2014;98:562-566.

20. Fadool JM, Dowling JE. Zebrafish: a model system for the study of eye genetics. *Prog Retin Eye Res*. 2008;27:89-110.

21. Glass AS, Dahm R. The zebrafish as a model organism for eye development. *Ophthalmic Res*. 2004;36:4-24.

22. Aose M, Linbo TH, Lawrence O, Senoo T, Raible DW, Clark JI. The occhiolino (occ) mutant Zebrafish, a model for development of the optical function in the biological lens. *Dev Dyn*. 2017;246:915-924.

23. Cavodeassi F, Wilson SW. Looking to the future of zebrafish as a model to understand the genetic basis of eye disease. *Hum Genet*. 2019;138:993-1000.

24. Dill H, Fischer U. Gene knockdown in zebrafish (Danio rerio) as a tool to model photoreceptor diseases. *Methods Mol Biol*. 2019;1834:209-219.

25. Gestri G, Link BA, Neuhauss SCF. The visual system of zebrafish and its use to model human ocular diseases. *Dev Neurobiol*. 2012;72:302-327.

26. Posner M, McDonald MS, Murray KL, Kiss AJ. Why does the zebrafish cloche mutant develop lens cataract? *PLoS One*. 2019;14:1-16.

27. Richardson R, Tracey-White D, Webster A, Moosajee M. The zebrafish eye-a paradigm for investigating human ocular genetics. *Eye*. 2017;31:68-86.

28. Santoriello C, Zon LI, Santoriello C, Zon LI. Hooked ! Modeling human disease in zebrafish Find the latest version: science in medicine Hooked ! Modeling human disease in zebrafish. *J Clin Invest*. 2012;122:2337-2343.

29. Lin HJ, Hong ZY, Li YK, Liau I. Fluorescent tracer of dopamine enables selective labelling and interrogation of dopaminergic amacrine cells in the retina of living zebrafish. *RSC Adv*. 2016;6:71589-71595.

30. Ma M, Ramirez AD, Wang T, et al. (2019) Zebrafish Dscaml1 is essential for retinal patterning and function of oculomotor subcircuits. *bioRxiv* 658161.

31. Mochizuki T, Masai I. The lens equator: a platform for molecular machinery that regulates the switch from cell proliferation to differentiation in the vertebrate lens. *Dev Growth Differ*. 2014;56:387-401.

32. Vacaru AM, Unlu G, Spitzner M, Mione M, Knapik EW, Sadler KC. In vivo cell biology in zebrafish - providing insights into vertebrate development and disease. *J Cell Sci*. 2014;127:485-495.

33. Kitambi SS, McCulloch KJ, Peterson RT, Malicki JJ. Small molecule screen for compounds that affect vascular development in the zebrafish retina. *Mech Dev*. 2009;126:464-477.

34. Stewart AM, Braubach O, Spitsbergen J, Gerlai R, Kalueff AV. Zebrafish models for translational neuroscience research: from tank to bedside. *Trends Neurosci*. 2014;37:264-278.

35. Ward R, Ali Z, Slater K, Reynolds AL, Jensen LD, Kennedy BN. Pharmacological restoration of visual function in a zebrafish model of von-Hippel Lindau disease. *Dev Biol*. 2020;457:226-234.

36. Zon LI, Peterson RT. In vivo drug discovery in the zebrafish. *Nat Rev Drug Discov*. 2005;4:35-44.

37. Del Bene F, Ettwiller L, Skowronska-Krawczyk D, et al. In vivo validation of a computationally predicted conserved Ath5 target gene set. *PLoS Genet*. 2007;3:1661-1671.

38. Paolini A, Duchemin AL, Albadri S, et al. Asymmetric inheritance of the apical domain and self-renewal of retinal ganglion cell progenitors depend on Anillin function. *Development*. 2015;142:832-839.

39. Jusuf PR, Albadri S, Paolini A, et al. Biasing amacrine subtypes in the Atoh7 lineage through expression of barhl2. *J Neurosci*. 2012;32:13929-13944.

40. Kimmel CB, Ballard WW, Kimmel SR, Ullmann B, Schilling TF. Stages of embryonic development of the zebrafish. *Dev Dyn*. 1995;203:253-310.

41. McNabb A, Scott K, Ochsenstein EV, Seufert K, Carl M. Don't be afraid to set up your fish facility. *Zebrafish*. 2012;9:120-125.

42. Masai I, Stemple DL, Okamoto H, Wilson SW. Midline signals regulate retinal neurogenesis in zebrafish. *Neuron*. 2000;27:251-263.

43. Weidinger G, Thorpe CJ, Wuennenberg-Stapleton K, Ngai J, Moon RT. The Sp1-related transcription factors sp5 and sp5-like act downstream of Wnt/β-catenin signaling in mesoderm and neuroectoderm patterning. *Curr Biol*. 2005;15:489-500.

44. Flicek P, Ahmed I, Amode MR,, et al. (2013) Ensembl 2013. *Nucleic Acids Res*. 41(D1):D48-D55.

45. Johnson WE, Li C, Rabinovic A. Adjusting batch effects in microarray expression data using empirical Bayes methods. *Biostatistics*. 2007;8:118-127.

46. Ritchie ME, Phipson B, Wu D, et al. Limma powers differential expression analyses for RNA-sequencing and microarray studies. *Nucleic Acids Res*. 2015;43:e47.

47. Durinck S, Spellman PT, Birney E, Huber W. Mapping identifiers for the integration of genomic datasets with the R/ Bioconductor package biomaRt. *Nat Protoc*. 2009;4:1184-1191.

48. Zhou Y, Zhou B, Pache L, et al. Metascape provides a biologist-oriented resource for the analysis of systems-level datasets. *Nature Commun*. 2019;10(1):1-10.

49. Xie C, Mao X, Huang J, et al. KOBAS 2.0: a web server for annotation and identification of enriched pathways and diseases. *Nucleic Acids Res*. 2011;39:W316-W322.

50. Szklarczyk D, Gable AL, Lyon D, et al. STRING v11: protein-protein association networks with increased coverage, supporting functional discovery in genome-wide experimental datasets. *Nucleic Acids Res*. 2019;47:D607-D613.

51. Shannon P, Markiel A, Ozier O, et al. Cytoscape: a software Environment for integrated models of biomolecular interaction networks. *Genome Res*. 2003;13:2498-2504.

52. Langfelder P, Horvath S. WGCNA: an R package for weighted correlation network analysis. *BMC Bioinformatics*. 2008;9(1):1-32.

53. Newman MEJ. Finding community structure in networks using the eigenvectors of matrices. *Phys Rev E*. 2006;74(3 Pt 2).036104

54. Schindelin J, Arganda-Carreras I, Frise E, et al. Fiji: an open-source platform for biological-image analysis. *Nat Methods*. 2012;9:676-682.

55. Hu M, Easter J. Retinal neurogenesis: the formation of the initial central patch of postmitotic cells. *Dev Biol*. 1999;207:309-321.

56. Gavriouchkina D, Fischer S, Ivacevic T, Stolte J, Benes V, Dekens MPS. Thyrotroph embryonic factor regulates light-induced transcription of repair genes in zebrafish embryonic cells. *PLoS One*. 2010;5:1-10.

57. Tissir F, Goffinet AM. Atypical cadherins Celsr1-3 and planar cell polarity in vertebrates. *Prog Molecular Biol Trans Sci*. 2013;116:193-214.

58. Abouzeid H, Youssef MA, Bayoumi N, et al. RAX and anophthalmia in humans: evidence of brain anomalies. *Mol Vis*. 2012;18:1449-1456.

59. Cantu JA, Flowers GP, Topczewski J. Notum homolog plays a novel role in primary motor innervation. *J Neurosci*. 2013;33:2177-2187.

60. Foulquier F, Amyere M, Jaeken J, et al. TMEM165 deficiency causes a congenital disorder of glycosylation. *Am J Hum Genet*. 2012;91:15-26.

61. Piekny AJ, Maddox AS. The myriad roles of Anillin during cytokinesis. *Semin Cell Dev Biol*. 2010;21:881-891.

62. Diacou R, Zhao Y, Zheng D, Cvekl A, Liu W. Six3 and Six6 Are jointly required for the maintenance of multipotent retinal progenitors through both positive and negative regulation. *Cell Rep*. 2018;25:2510-2523.e4.

63. Loosli F, Staub W, Finger-Baier KC, et al. Loss of eyes in zebrafish caused by mutation of chokh/rx 3. *EMBO Rep*. 2003;4:894-899.

64. Nelson SM, Park L, Stenkamp DL. Retinal homeobox 1 is required for retinal neurogenesis and photoreceptor differentiation in embryonic zebrafish. *Dev Biol*. 2009;328:24-39.

65. Markitantova Y, Simirskii V. Inherited eye diseases with retinal manifestations through the eyes of homeobox genes. *Int J Mol Sci*. 2020;21:6-8.

66. Hehr CL, Hocking JC, McFarlane S. Matrix metalloproteinases are required for retinal ganglion cell axon guidance at select decision points. *Development*. 2005;132:3371-3379.

67. Janssens E, Gaublomme D, de Groef L, et al. Matrix metalloproteinase 14 in the zebrafish: an eye on retinal and retinotectal development. *PLoS One*. 2013;8:e52915.

68. Lemmens K, Bollaerts I, Bhumika S, et al. Matrix metalloproteinases as promising regulators of axonal regrowth in the injured adult zebrafish retinotectal system. *J Comp Neurol*. 2016;524:1472-1493.

69. Piri N, Kwong JMK, Gu L, Caprioli J. Heat shock proteins in the retina: focus on HSP70 and alpha crystallins in ganglion cell survival. *Prog Retin. Eye Res*. 2016;52:22-46.

70. Cvekl A, Mitton KP. Epigenetic regulatory mechanisms in vertebrate eye development and disease. *Heredity (Edinb)*. 2010;105:135-151.

71. Scheidecker S, Etard C, Haren L, et al. Mutations in TUBGCP4 alter microtubule organization via the γ-tubulin ring complex in autosomal-recessive microcephaly with chorioretinopathy. *Am J Hum Genet*. 2015;96:666-674.

72. Blixt MKE, Konjusha D, Ring H, Hallböök F. Zinc finger gene nolz1 regulates the formation of retinal progenitor cells and suppresses the Lim3/Lhx3 phenotype of retinal bipolar cells in chicken retina. *Dev Dyn*. 2018;247:630-641.

73. Paridaen JTML, Janson E, Utami KH, et al. The nucleolar GTP-binding proteins Gnl2 and nucleostemin are required for retinal neurogenesis in developing zebrafish. *Dev Biol*. 2011;355:286-301.

74. Agathocleous M, Harris WA. From progenitors to differentiated cells in the vertebrate retina. *Annu Rev Cell Dev Biol*. 2009;25:45-69.

75. Zhang L, Maddox AS. Anillin. *Curr Biol*. 2010;20(4):R135-R136.

76. Malo MC, Duchemin AL, Guglielmi L, et al. The zebrafish anillin-eGFP reporter marks late dividing retinal precursors and stem cells entering neuronal lineages. *PLoS One*. 2017;12:e0170356.

77. Pandi NS, Manimuthu M, Harunipriya P, Murugesan M, Asha GV, Rajendran S. In silico analysis of expression pattern of a Wnt/β-catenin responsive gene ANLN in gastric cancer. *Gene*. 2014;545:23-29.

78. Meyers JR, Hu L, Moses A, Kaboli K, Papandrea A, Raymond PA. β-catenin/Wnt signaling controls progenitor fate in the developing and regenerating zebrafish retina. *Neural Dev*. 2012;7(1):30.

79. Alizadeh E, Mammadzada P, André H. The different facades of retinal and choroidal endothelial cells in response to hypoxia. *Int J Mol Sci*. 2018;19:3846.

80. Reinhardt R, Centanin L, Tavhelidse T, et al. Sox2, Tlx, Gli3, and Her9 converge on Rx2 to define retinal stem cells in vivo. *EMBO J*. 2015;34:1572-1588.

81. Furukawa T, Kozak CA, Cepko CL. rax, a novel paired-type homeobox gene, shows expression in the anterior neural fold and developing retina. *Proc Natl Acad Sci U SA*. 1997;94:3088-3093.

82. Loosli F, Winkler S, Burgtorf C, et al. Medaka eyeless is the key factor linking retinal determination and eye growth. *Development*. 2001;128:4035-4044.

83. Mathers PH, Grinberg A, Mahon KA, Jamrich M. The Rx homeobox gene is essential for vertebrate eye development. *Nature*. 1997;387:603-607.

84. Chassaing N, Causse A, Vigouroux A, et al. Molecular findings and clinical data in a cohort of 150 patients with anophthalmia/microphthalmia. *Clin Genet*. 2014;86:326-334.

85. Lequeux L, Rio M, Vigouroux A, et al. Confirmation of RAX gene involvement in human anophthalmia. *Clin Genet*. 2008;74:392-395.

86. Voronina VA, Kozhemyakina EA, O'Kernick CM, et al. Mutations in the human RAX homeobox gene in a patient with anophthalmia and sclerocornea. *Hum Mol Genet*. 2004;13:315-322.

87. Aldahmesh MA, Khan AO, Hijazi H, Alkuraya FS. Homozygous truncation of SIX6 causes complex microphthalmia in humans. *Clin Genet*. 2013;84:198-199.

88. Teotia P, Van Hook MJ, Wichman CS, Allingham RR, Hauser MA, Ahmad I. Modeling glaucoma: retinal ganglion cells

generated from induced pluripotent stem cells of patients with SIX6 risk allele show developmental abnormalities. *Stem Cells*. 2017;35:2239-2252.

89. Chen Y, Hughes G, Chen X, et al. Genetic variants associated with different risks for high tension glaucoma and normal tension glaucoma in a Chinese population. *Investig Ophthalmol Vis Sci*. 2015;56:2595-2600.

90. Khawaja AP, Cooke Bailey JN, Wareham NJ, et al. Genome-wide analyses identify 68 new loci associated with intraocular pressure and improve risk prediction for primary open-angle glaucoma. *Nat Genet*. 2018;50:778-782.

91. Mabuchi F, Sakurada Y, Kashiwagi K, Yamagata Z, Iijima H, Tsukahara S. Involvement of genetic variants associated with primary open-angle glaucoma in pathogenic mechanisms and family history of glaucoma. *Am J Ophthalmol*. 2015;159:437-444.e2.

92. Yariz KO, Sakalar YB, Jin X, et al. A homozygous SIX6 mutation is associated with optic disc anomalies and macular atrophy and reduces retinal ganglion cell differentiation. *Clin Genet*. 2015;87:192-195.

93. Abu-Amero K, Kondkar AA, Chalam KV. An updated review on the genetics of primary open angle glaucoma. *Int J Mol Sci*. 2015;16:28886-28911.

94. Philomenadin FS, Asokan R, Viswanathan N, George R, Lingam V, Sarangapani S. Genetic association of SNPs near ATOH7, CARD10, CDKN2B, CDC7 and SIX1/SIX6 with the endophenotypes of primary open angle glaucoma in Indian Population. *PLoS One*. 2015;10:e0119703.

95. Khan AO. Genetics of primary glaucoma. *Curr Opin Ophthalmol*. 2011;22:347-355.

96. Reis LM, Semina EV. Conserved genetic pathways associated with microphthalmia, anophthalmia, and coloboma. *Birth Defects Res Part C - Embryo Today Rev*. 2015;105:96-113.

97. Goodwin LR, Picketts DJ. The role of ISWI chromatin remodeling complexes in brain development and neurodevelopmental disorders. *Mol Cell Neurosci*. 2018;87:55-64.

98. Das AV, James J, Bhattacharya S, et al. SWI/SNF chromatin remodeling ATPase Brm regulates the differentiation of early retinal stem cells/progenitors by influencing Brn3b expression and Notch signaling. *J Biol Chem*. 2007;282:35187-35201.

99. He S, Limi S, McGreal RS, et al. Chromatin remodeling enzyme Snf2h regulates embryonic lens differentiation and denucleation. *Dev*. 2016;143:1937-1947.

100. Gross JM, Perkins BD, Amsterdam A, et al. Identification of Zebrafish insertional mutants with defects in visual system development and function. *Genetics*. 2005;170:245-261.

101. Martins D, Moreira J, Gonçalves NP, Saraiva MJ. MMP-14 overexpression correlates with the neurodegenerative process in familial amyloidotic polyneuropathy. *DMM Dis Model Mech*. 2017;10:1253-1260.

102. Nagashima M, Fujikawa C, Mawatari K, Mori Y, Kato S. HSP70, the earliest-induced gene in the zebrafish retina during optic nerve regeneration: its role in cell survival. *Neurochem Int*. 2011;58:888-895.

103. Fujikawa C, Nagashima M, Mawatari K, Kato S. HSP70 gene expression in the zebrafish retina after optic nerve injury: a comparative study under heat shock stresses. *Adv Exp Med Biol*. 2012;723:663-668.

104. Sinha D, Klise A, Sergeev Y, et al. βA3/A1-crystallin in astroglial cells regulates retinal vascular remodeling during development. *Mol Cell Neurosci*. 2008;37:85-95.

105. Drankowska J, Kos M, Kościuk A, et al. MMP targeting in the battle for vision: recent developments and future prospects in the treatment of diabetic retinopathy. *Life Sci*. 2019;229:149-156.

106. Kubo F, Takeichi M, Nakagawa S. Wnt2b inhibits differentiation of retinal progenitor cells in the absence of Notch activity by downregulating the expression of proneural genes. *Development*. 2005;132:2759-2770.

107. Masai I, Yamaguchi M, Tonou-Fujimori N, Komori A, Okamoto H. The hedgehog-PKA pathway regulates two distinct steps of the differentiation of retinal ganglion cells: The cell-cycle exit of retinoblasts and their neuronal maturation. *Development*. 2005;132:1539-1553.

108. Souren M, Martinez-Morales JR, Makri P, Wittbrodt B, Wittbrodt J. A global survey identifies novel upstream components of the Ath5 neurogenic network. *Genome Biol*. 2009;10.

109. Gao Z, Mao CA, Pan P, Mu X, Klein WH. Transcriptome of Atoh7 retinal progenitor cells identifies new Atoh7-dependent regulatory genes for retinal ganglion cell formation. *Dev Neurobiol*. 2014;74:1123-1140.

110. Shima Y, Kawaguchi SY, Kosaka K, et al. Opposing roles in neurite growth control by two seven-pass transmembrane cadherins. *Nat Neurosci*. 2007;10:963-969.

111. Hackam AS. The Wnt signaling pathway in retinal degenerations. *IUBMB Life*. 2005;57:381-388.

112. Poggi L, Casarosa S, Carl M. An eye on the WNT inhibitory factor Wif1. *Front Cell Dev Biol*. 2018;6:167 -174.

113. Shastry BS. Persistent hyperplastic primary vitreous: congenital malformation of the eye. *Clin Exp Ophthalmol*. 2009;37:884-890.

114. Bats ML, Bougaran P, Peghaire C, et al. Therapies targeting Frizzled-7/β-catenin pathway prevent the development of pathological angiogenesis in an ischemic retinopathy model. *FASEB J*. 2020;34:1288-1303.

115. Fujimura N. WNT/β-catenin signaling in vertebrate eye development. *Front Cell Dev Biol*. 2016;4.

116. Mills EA, Goldman D. The regulation of notch signaling in retinal development and regeneration. *Curr Pathobiol Rep*. 2017;5:323-331.

117. Chiodini F, Matter-Sadzinski L, Rodrigues T, et al. A positive feedback loop between ATOH7 and a notch effector regulates cell-cycle progression and neurogenesis in the retina. *Cell Rep*. 2013;3:796-807.

118. Song W-T, Zeng QI, Xia X-B, Xia K, Pan Q. Atoh7 promotes retinal Müller cell differentiation into retinal ganglion cells. *Cytotechnology*. 2016;68:267-277.

119. Nelson BR, Gumuscu B, Hartman BH, Reh TA. Notch activity is downregulated just prior to retinal ganglion cell differentiation. *Dev Neurosci*. 2006;28:128-141.

120. Ohnuma SI, Hopper S, Wang KC, Philpott A, Harris WA. Coordinating retinal histogenesis: early cell cycle exit enhances early cell fate determination in the Xenopus retina. *Development*. 2002;129:2435-2446.

121. Del Bene F, Wehman AM, Link BA, Baier H. Regulation of neurogenesis by interkinetic nuclear migration through an apical-basal notch gradient. *Cell*. 2008;134:1055-1065.

122. Wu F, Kaczynski TJ, Sethuramanujam S, et al. Two transcription factors, Pou4f2 and Isl1, are sufficient to specify the retinal ganglion cell fate. *Proc Natl Acad Sci USA*. 2015;112:E1559-E1568.

123. Dai X, Chen X, Hakizimana O, Mei Y. Genetic interactions between ANLN and KDR are prognostic for breast cancer survival. *Oncol Rep*. 2019;42:2255-2266.

124. Gbadegesin RA, Hall G, Adeyemo A, et al. Mutations in the gene that encodes the F-Actin binding protein anillin cause FSGS. *J Am Soc Nephrol*. 2014;25:1991-2002.

125. Hall G, Lane BM, Khan K, et al. The human FSGS-causing ANLN R431C mutation induces dysregulated PI3K/AKT/mTOR/Rac1 signaling in podocytes. *J Am Soc Nephrol*. 2018;29:2110-2122.

126. Lian YF, Huang YL, Wang JL, et al. Anillin is required for tumor growth and regulated by miR-15a/miR- 16–1 in HBV-related hepatocellular carcinoma. *Aging (Albany. NY)*. 2018;10:1884-1901.

127. Tian D, Diao M, Jiang Y, et al. Anillin regulates neuronal migration and neurite growth by linking RhoG to the actin cytoskeleton. *Curr Biol*. 2015;25:1135-1145.

128. Rehain K, Maddox AS. Neuron migration: anillin protects leading edge actin. *Curr Biol*. 2015;25:R423-R425.

129. Erwig MS, Patzig J, Steyer AM, et al. Anillin facilitates septin assembly to prevent pathological outfoldings of central nervous system myelin. *Elife*. 2019;8.

130. Patzig J, Erwig MS, Tenzer S, et al. Septin/anillin filaments scaffold central nervous system myelin to accelerate nerve conduction. *eLife*. 2016;5:e17119.

131. Fagotto F. Looking beyond the Wnt pathway for the deep nature of β-catenin. *EMBO Rep*. 2013;14:422-433.

132. Tian X, Liu Z, Niu B, et al. E-Cadherin/β-catenin complex and the epithelial barrier. *J Biomed Biotechnol*. 2011;2011:567305.

133. Nusse R, Clevers H. Wnt/β-catenin signaling, disease, and emerging therapeutic modalities. *Cell*. 2017;169:985-999.

134. Yao K, Qiu S, Tian L, et al. Wnt regulates proliferation and neurogenic potential of müller glial cells via a Lin28/let-7 miRNA-dependent pathway in adult mammalian retinas. *Cell Rep*. 2016;17:165-178.

135. Smith JR, David LL, Appukuttan B, Wilmarth PA. Angiogenic and immunologic proteins identified by deep proteomic profiling of human retinal and choroidal vascular endothelial cells: potential targets for new biologic drugs. *Am J Ophthalmol*. 2018;193:197-229.

136. Weger BD, Sahinbas M, Otto GW, et al. The light responsive transcriptome of the Zebrafish: function and regulation. *PLoS One*. 2011;6:e17080.

137. Baba K, Piano I, Lyuboslavsky P, et al. Removal of clock gene Bmal1 from the retina affects retinal development and accelerates cone photoreceptor degeneration during aging. *Proc Natl Acad Sci USA*. 2018;115:13099-13104.

138. Stone RA, McGlinn AM, Chakraborty R, et al. Altered ocular parameters from circadian clock gene disruptions. *PLoS One*. 2019;14(6):e0217111.

139. Sawant OB, Jidigam VK, Fuller RD, et al. The circadian clock gene Bmal1 is required to control the timing of retinal neurogenesis and lamination of Müller glia in the mouse retina. *FASEB J*. 2019;33:8745-8758.

140. Laranjeiro R, Whitmore D. Transcription factors involved in retinogenesis are co-opted by the circadian clock following photoreceptor differentiation. *Development*. 2014;141:2644-2656.

141. Felder-Schmittbuhl M-P, Calligaro H, Dkhissi-Benyahya O. The retinal clock in mammals: role in health and disease. *ChronoPhysiology Ther*. 2017;7:33-45.

SUPPORTING INFORMATION

Additional supporting information may be found online in the Supporting Information section.